

**THERMAL STUDIES ON SODIUM SILICATE HYDRATES. II.
DISODIUM DIHYDROGENSILICATE HYDRATES,
 $\text{Na}_2\text{H}_2\text{SiO}_4 \cdot n \text{H}_2\text{O}$ ($n = 4, 5, 7, 8$); MELTING
CHARACTERISTICS AND SOLIDIFICATION OF
GLASSLIKE HYDRATE PHASES AT LOW TEMPERATURES**

J. FELSCHE, B. KETTERER and R.L. SCHMID

Fakultät für Chemie, Universität Konstanz, Postfach 5560, D-7750 Konstanz (F.R.G.)

Received 10 January 1984)

ABSTRACT

Thermoanalytical studies on the compounds $\text{Na}_2\text{H}_2\text{SiO}_4 \cdot n \text{H}_2\text{O}$ ($n = 4, 5, 7, 8$) reveal congruent melting of all four members of the 1:1 hydrate series, which is contrary to the corresponding 3:2 hydrate series $\text{Na}_3\text{HSiO}_4 \cdot n \text{H}_2\text{O}$ ($n = 5, 2, 1, 0$) or intercalation type compounds $\text{Na}_{2-x}\text{H}_x\text{Si}_2\text{O}_5 \cdot n \text{H}_2\text{O}$, which definitely melt incongruently and which show stepwise dehydration at elevated temperatures due to peritectical decomposition. The unique melting behaviour of the 1:1 hydrates, which obviously correlates to the intensive hydrogen bonding around the special $[\text{SiO}_2(\text{OH})_2]^{2-}$ anion, is furthermore distinguished by irreversibility of the phase transitions. This irreversible melting of the 1:1 hydrates subsequently yields typical liquid or viscous waterglass phases upon cooling from melting temperatures at 351, 341, 325 and 323 K above room temperature. T_g values of solidification at low temperatures, 227, 234, 255 and 264 K, correspond linearly to the reciprocal number of hydrate water molecules $n \text{H}_2\text{O}$ or to the reciprocal molecular weight M^{-1} of the individual 1:1 silicate hydrate phases. From DSC characteristics or structural arguments on the special hydrogen bonding features from neutron diffraction data, amorphous phases of this group of silicate hydrates closely correspond to the well-known organic polymeric materials of chalcogenide type glasses. Deviations of melting data due to different experimental conditions are discussed. Special melting features from heating experiments of X-ray diffraction or polarization microscopy are supplied.

INTRODUCTION

Disodium dihydrogenorthosilicate hydrates $\text{Na}_2\text{H}_2\text{SiO}_4 \cdot n \text{H}_2\text{O}$ ($n = 4, 5, 7, 8$) dominate the system $\text{Na}_2\text{O}-\text{SiO}_2-\text{H}_2\text{O}$ in respect to their industrial importance in alkali and silicate chemistry. Data on thermal properties of the materials are of special interest for production processes, storage qualities and secondary refinement or exchange properties in various applications.

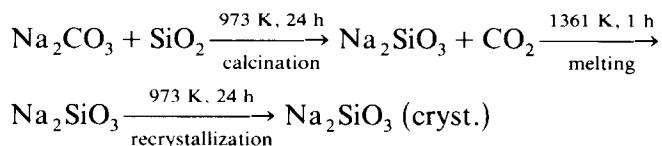
From the viewpoint of fundamental science more needs to be known about the unique anion $[\text{SiO}_2(\text{OH})_2]^{2-}$ which is, so far, known to exist

exclusively in this hydrate series. Of special interest are correlations between structural and thermal properties of water-rich hydrate phases. Since our knowledge of special hydrogen bonding schemes has been confirmed through neutron diffraction data on $\text{Na}_2\text{H}_2\text{SiO}_4 \cdot 5 \text{H}_2\text{O}$ [1], $\text{Na}_2\text{D}_2\text{SiO}_4 \cdot 8 \text{D}_2\text{O}$ [2] and $\text{Na}_2\text{H}_2\text{SiO}_4 \cdot 4 \text{H}_2\text{O}$ [3], we now want to provide complete and accurate data on the thermal properties of all four hydrate phases within the 1:1 sodium silicate hydrate series. Therefore, the recently reported data on melting are given for polycrystalline samples of the corresponding tetra-, penta- and octa-hydrate [4]. The report on special sorption properties of the disodium dihydrogen orthosilicate hydrates will be continued in a later paper.

EXPERIMENTAL

Pure phase single crystal qualities of all four hydrates $\text{Na}_2\text{H}_2\text{SiO}_4 \cdot n \text{H}_2\text{O}$ ($n = 4, 5, 7, 8$) have been grown by different approaches of various crystal growth techniques. Special single crystal qualities several millimetres in size have been selected due to the demands of neutron diffraction experiments. Smaller fractions or twinned material have been supplied for the corresponding study on thermal properties of the 1:1 hydrates here.

Employing high grade Na_2CO_3 (Merck 6392E) and $\text{SiO}_2 \cdot n \text{H}_2\text{O}$ (Merck 657) as starting materials, pure phase metasilicate Na_2SiO_3 was obtained through the following sequence of reactions.



Compact samples of polycrystalline metasilicate were ground to particle sizes of 25–50 μm for subsequent hydrolysis at elevated temperatures under CO_2 -free but open system conditions (Braun glovebox M20). Single crystals of the octahydrate, up to 20 mm in size, have been grown from nearly stoichiometric solutions (6.5% Na_2O , 6.2% SiO_2 , 87.3% H_2O) and those of the tetrahydrate with considerable excess of NaOH (45% Na_2O , 10% SiO_2 , 45% H_2O) at temperatures of 298 K after the addition of small fractions of seeds from selected samples of pure phase material. Crystals of $\text{Na}_2\text{H}_2\text{SiO}_4 \cdot 5 \text{H}_2\text{O}$ have been obtained from solutions of 20.50% Na_2O , 9.80% SiO_2 , 69.70% H_2O at 291 K and those of $\text{Na}_2\text{H}_2\text{SiO}_4 \cdot 7 \text{H}_2\text{O}$ from 11.19% Na_2O , 11.53% SiO_2 , 76.92% H_2O at temperatures of 298 K under CO_2 -free atmosphere. All concentrations are given in wt.%.

The constitution of polycrystalline or single crystal phases has been proved by X-ray diffraction Guinier or precession techniques, polarization microscopy and thermogravimetry (Netzsch STA 429).

In order to verify influences from sample geometry on the calorimetric data, hydrate samples were provided in two qualities for differential scanning calorimetry (Perkin-Elmer DSC 2). Single crystals (~ 5 mg) were selected from the individual batches, meeting the dimensions of the DSC sample capsules (diameter = 6 mm, height = 2 mm). Polycrystalline samples (25–50 μm) of identical phases were chosen for additional experiments in order to quantify deviations from ideal melting conditions. With the given set of polycrystalline samples it is necessary to control boundary effects from large specific surfaces, which are known to affect phase transitions of hydrates, because of their considerable (H_2O) partial pressure. The grinding of samples was avoided, where possible, in order to prevent any tribochemical effect on thermal data. Furthermore, precautions were taken to prevent any CO_2 or H_2O sorption to or from samples, respectively by supplying an N_2 - or Ar-protection atmosphere for any analytical procedure.

DSC experiments were carried out at temperatures of 100–500 K employing liquid nitrogen at temperatures below room temperature. Temperature standards were provided by compact indium (m.p. 429.78 K) and cyclohexane (m.p. 186.1 K). The enthalpy of fusion of In ($\Delta H = 3.271 \text{ kJ mol}^{-1}$) served as calorimetric standard. Silver pan bases and tightly sealed lids provided the best closed system conditions to temperatures of 450 K found by water pressure test experiments. Helium atmosphere (99.999%) was provided for open system conditions employing the same type of silver pans and lids, this time unsealed, in order to supply identical or nearly identical conditions of thermal conductivity.

Melting characteristics have also been studied by X-ray Guinier powder diffraction heating photographs or polarization microscopy employing heating stage equipment (Leitz, Wetzlar).

RESULTS AND DISCUSSION

Differential scanning calorimetry, X-ray heating diffraction and polarization microscopy unambiguously reveal the congruent melting character for all four hydrate phases $\text{Na}_2\text{H}_2\text{SiO}_4 \cdot n \text{H}_2\text{O}$ ($n = 4, 5, 7, 8$; Figs. 1–3).

Furthermore, the DSC data in Fig. 1 suggest irreversibility of the phase transition solid (crystalline) \rightarrow (homogeneous) melt which is confirmed by microscopic photographs at elevated temperatures (Fig. 2). Recrystallization was not observed during continuous solidification of the melt at temperatures as low as 100 K under closed system conditions allowing for any cooling rate. Data are excluded on recrystallization of liquid melts or solid hydrate phases during open system experimental conditions or decomposition reactions controlled by sorption effects. This will be reported later.

Solidification of hydrate melts occurs at rather low temperatures yielding glass temperatures, T_g , of 227, 234, 255 or 264 K for the octa-, hepta-, penta-

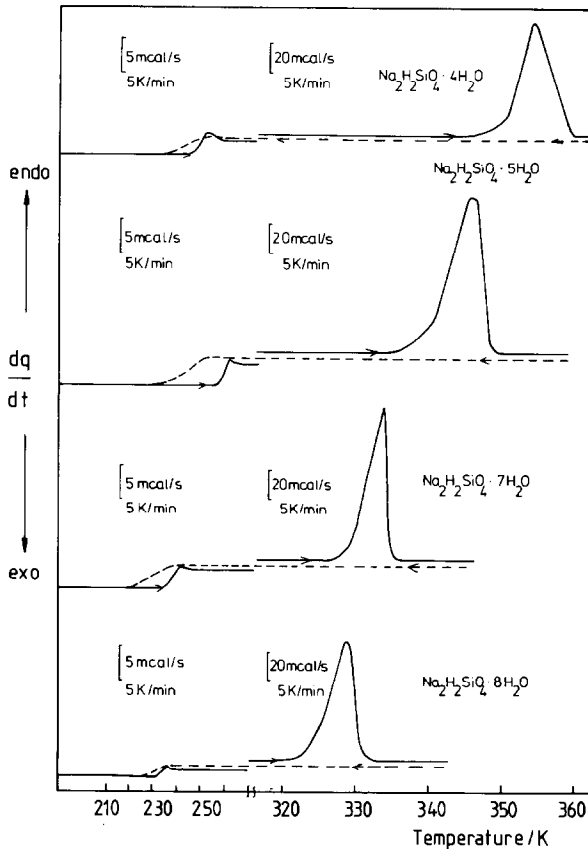


Fig. 1. DSC patterns of the phases $\text{Na}_2\text{H}_2\text{SiO}_4 \cdot n \text{H}_2\text{O}$ ($n = 4, 5, 7, 8$) at temperatures of 200–360 K. Single crystals in sealed silver capsules were heated to elevated temperatures at 5 K min^{-1} . Melting points of individual phases were passed over by ~ 10 K. No recrystallization peak has ever been observed on subsequent cooling of the melts as far down as ~ 100 K under various heating conditions. Solidification of the melts, however, occurs at temperatures beyond 273 K. A T_g of 264, 255, 234 and 227 K was provided from significant decays of the individual C_p curves of the tetra-, penta-, hepta- and octahydrate, respectively. It is this DSC transformation characteristic of amorphous solid \leftrightarrow viscous melt, which bears some resemblance to common silicate glasses or to the organic polymers. Individual runs had to be interrupted at room temperature, because of the liquid nitrogen supply for low temperature experiments.

or tetrahydrate, respectively, under closed system conditions (Fig. 4). Intervals of transition temperatures glass \leftrightarrow liquid melt show a maximum of about 30 K for the pentahydrate, which also yields the most pronounced decay of the C_p curve on cooling. On the other hand, melting points or glass temperatures show a rather uniform decrease with increasing number of water molecules per hydrate phase (Fig. 5).

Individual T_g values show a considerable linearity vs. reciprocal molecular weight M^{-1} (Fig. 6), which resembles the solidification characteristics of organic polymers like polyethylene or polystyrene.

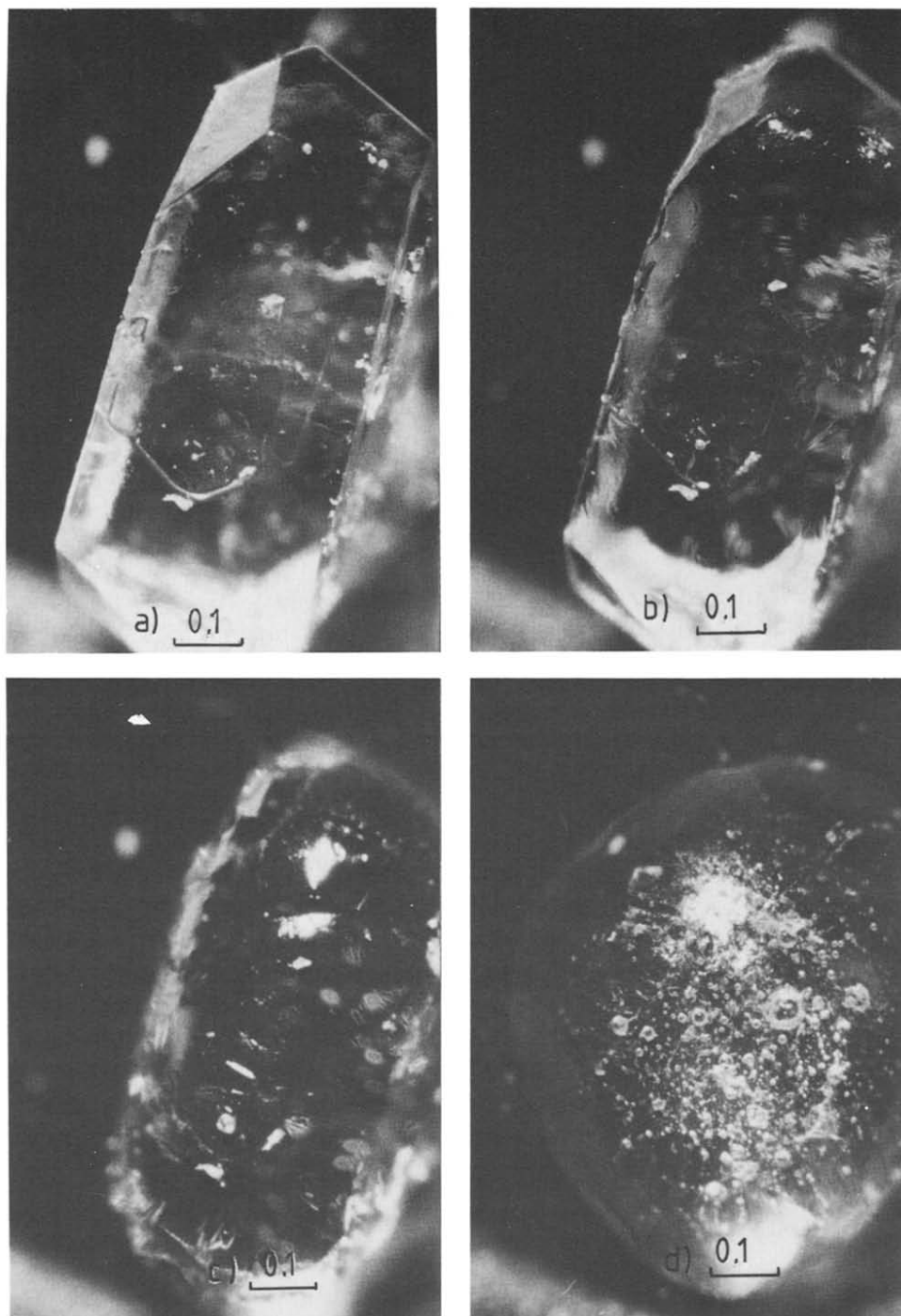


Fig. 2. Melting of a single crystal of $\text{Na}_2\text{H}_2\text{SiO}_4 \cdot 7 \text{H}_2\text{O}$ as observed by polarization microscopy (Leitz/Wild photomicroscope; Leitz heating stage). (a) The intact crystal 2 K below the melting temperature of 326 K; (b, c, d) confirm the congruent melting character of the heptahydrate at temperatures of 330, 400 and 450 K, respectively. Continuous contraction of the liquid melt provides the spherical shape of the material (d), which reveals its amorphous constitution from the optically isotropic character.

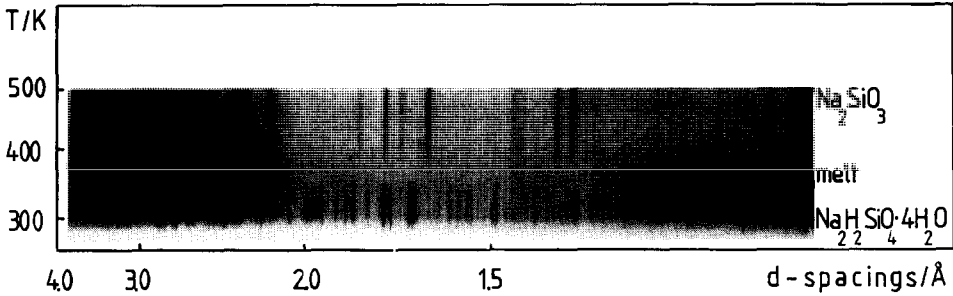


Fig. 3. X-Ray diffraction heating photograph of $\text{Na}_2\text{H}_2\text{SiO}_4 \cdot 4\text{H}_2\text{O}$ (Guinier technique; $\text{Cu K}\alpha_1$ radiation; heating rate: 5 K h^{-1} ; film feed: 0.75 mm h^{-1} ; polycrystalline sample in quartz tube, 5-mm I.D.). Any diffraction pattern missing at temperatures 357–370 K unambiguously confirms the congruent melting character of the compounds. Identical features have been obtained for the other three members of the series $\text{Na}_2\text{H}_2\text{SiO}_4 \cdot n\text{H}_2\text{O}$. This emphasizes the unique melting character of this group of hydrates as compared to the common (incongruent) melting behaviour of salt hydrates.

Structural arguments to explain this unique melting character of the 1:1 hydrates might be obtained qualitatively from Figs. 7 and 8. Structural details of the hydrogen bonding can be obtained from refs. 1–3. Common to all four hydrate phases is the tetrahedral $[\text{SiO}_2(\text{OH})_2]^{2-}$ anion. This is the rigid centre of subsequent tetrahedrally coordinated oxygens. All oxygen and hydrogen atoms of the given structures are involved in intensive hydrogen bonding. The most favourable type of coordination around the oxygens is of class 2A...E [5]. Thus, tetrahedral coordination of rigid salt-like constituents $[\text{SiO}_2(\text{OH})_2]^{2-}$ and of weaker ice-like $[\text{O}(\dots\text{H})_3\text{M}]^{n+}$ centres dominate the three-dimensional framework structures of all four hydrate phases. Sodium

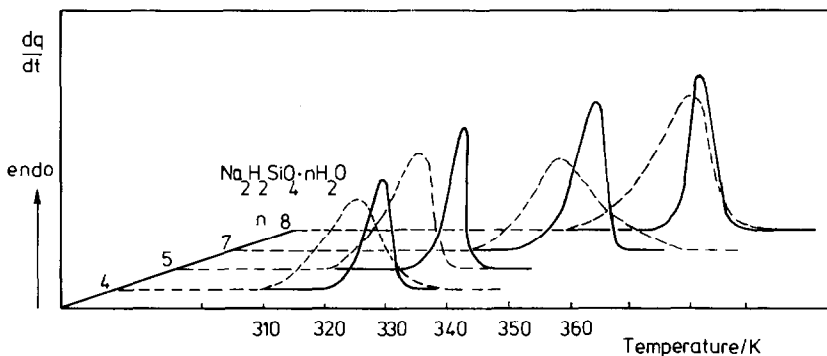


Fig. 4. DSC melting curves of hydrates $\text{Na}_2\text{H}_2\text{SiO}_4 \cdot n\text{H}_2\text{O}$ under open system conditions (5 K min^{-1} ; silver pans with lids; flowing gas: He 99.99%). The shape of the melting peaks, their areas and set points of single crystals (solid lines) seriously deviate from the corresponding curves of polycrystalline samples (grain size 25–50 μm). Reference is given to data in Table 1 or Fig. 1. This data unambiguously illustrates the necessary supply of closed system conditions for experiments on melting of compounds, which show considerable partial pressure at elevated temperatures.

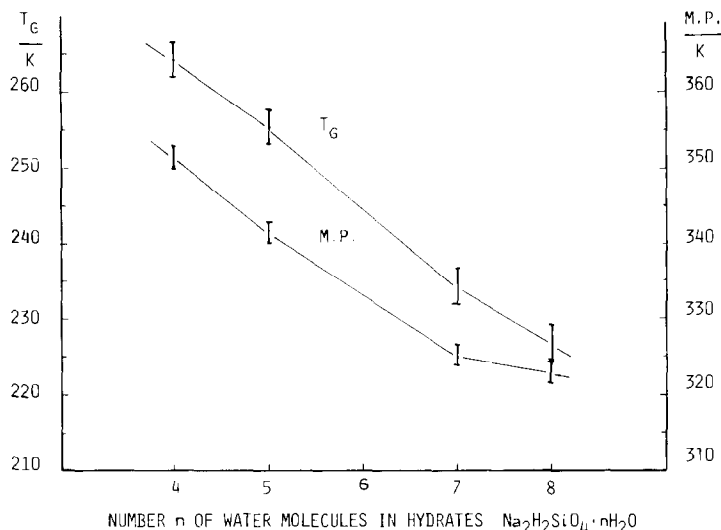


Fig. 5. Melting points (m.p.) or glass points (T_g) of disodium dihydrogensilicate hydrates and their dependence on concentrations n H_2O in hydrates $Na_2H_2SiO_4 \cdot nH_2O$. Values of m.p. and T_g decrease uniformly with increasing water contents.

atoms fill up the remaining cage-like volumes, which mostly provide sixfold oxygen coordination for the metal ions, M^+ .

Looking for further common structural features which might correlate to

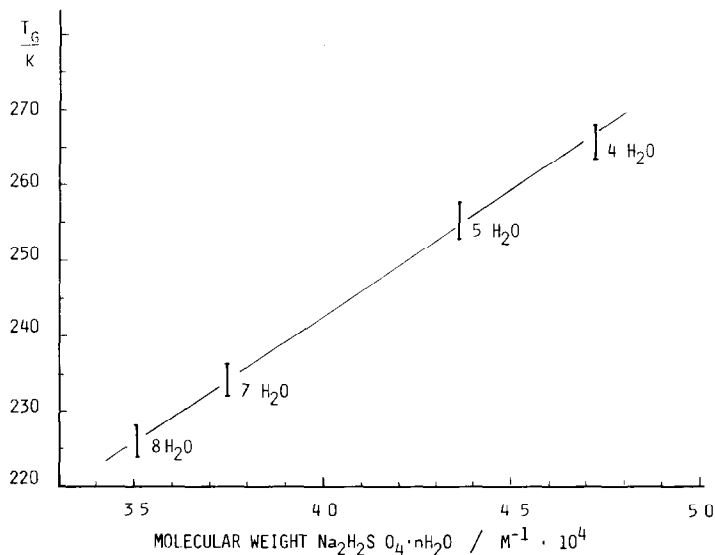


Fig. 6. Glass points, T_g , vs. reciprocal molecular weight, M^{-1} , of $Na_2H_2SiO_4 \cdot nH_2O$ hydrates ($n = 4, 5, 7, 8$). Considerable linearity of $T_g = f(M^{-1})$ reveals close correspondence of these inorganic amorphous hydrate materials to organic polymers, which also show increasing T_g values with increasing bonding strengths or conformation energies from lateral chains (e.g., polyethylene, polystyrole).

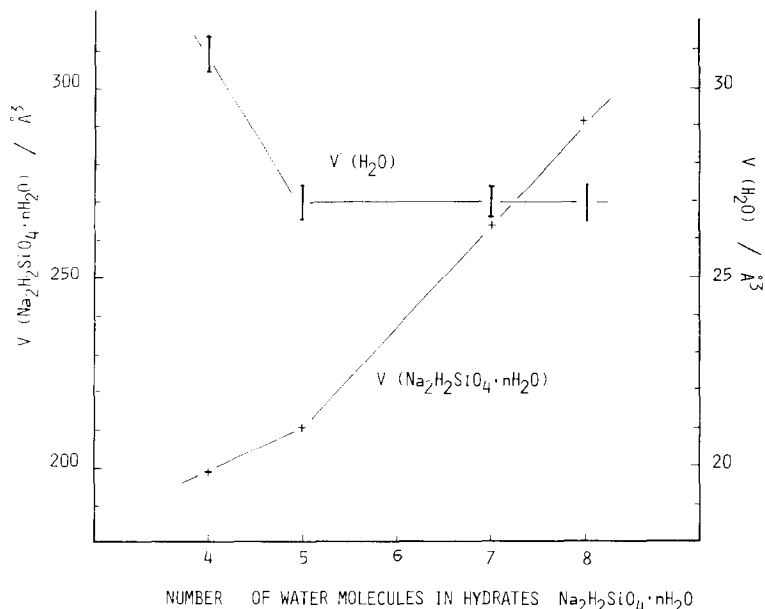
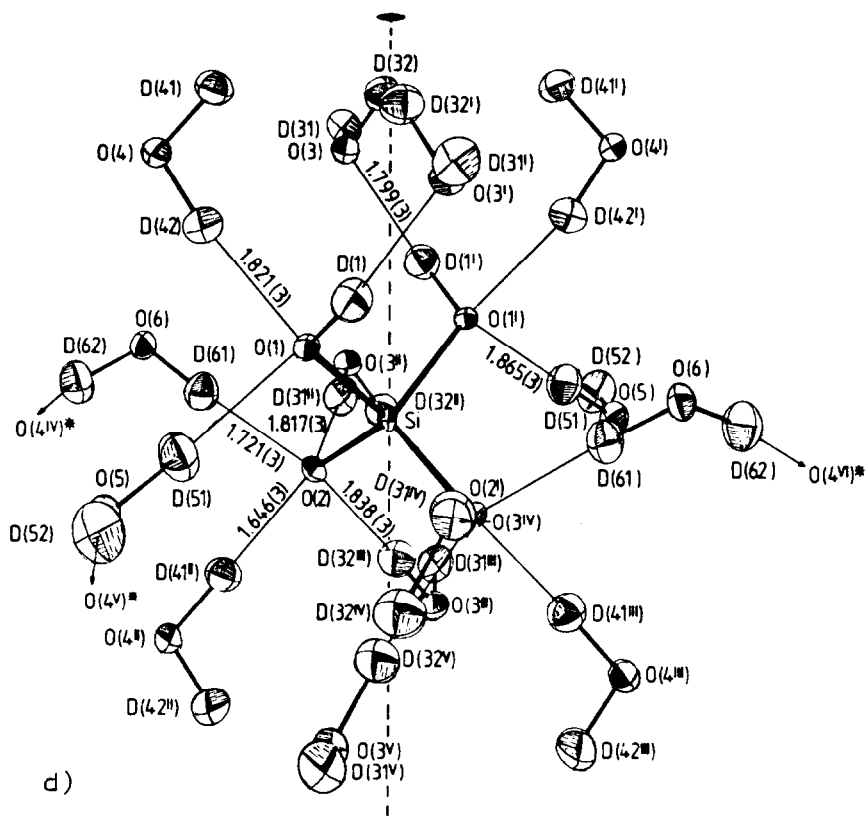
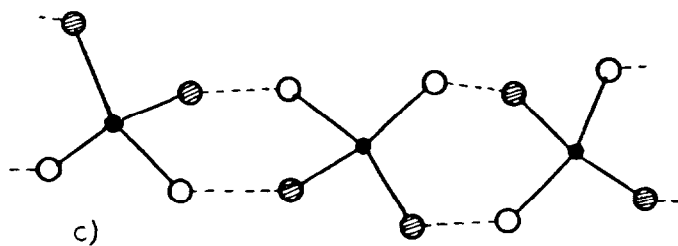
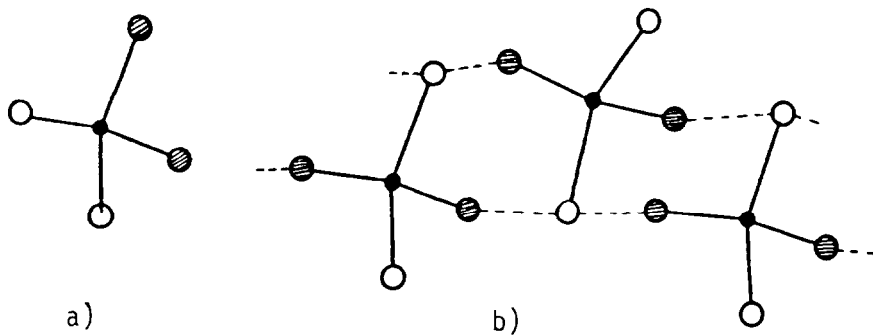


Fig. 7. Volume per formula unit $\text{Na}_2\text{H}_2\text{SiO}_4 \cdot n\text{H}_2\text{O}$ ($n = 4, 5, 7, 8$) or volume per molecule of H_2O ($V/\text{H}_2\text{O}$) vs. number, n , of hydrate water molecules present in each solid crystalline phase (data from X-ray powder diffraction Guinier $\text{Cu } K_{\alpha 1}$ photographs of pure phase material). The larger specific volume of $V/\text{H}_2\text{O} \approx 31 \text{ \AA}^3$ in the tetrahydrate as compared to $V/\text{H}_2\text{O} \approx 27 \text{ \AA}^3$ in the remaining silicate hydrates obviously corresponds to the unusual fivefold $\text{Na}(\text{H}_2\text{O} \cdot \text{OH} \cdot \text{O})_5$ coordination and the unique rigidity of endless silicate chains from edge-connected hydrogen bonded $[\text{Si}(\text{OH})_2\text{O}_2]^{2-}$ tetrahedra [3].

the unique melting behaviour of all four hydrates, a rather harmonic binding is assigned to the four different constituents in the structure, Na, Si, O and H, qualitatively. Figure 8 shows the essential part of the hydrogen bonding, which is mostly concentrated around the $[\text{SiO}_2(\text{OH})_2]^{2-}$ tetrahedra, within the structure of $\text{Na}_2\text{H}_2\text{SiO}_4 \cdot 8\text{H}_2\text{O}$ [2]. All the sodium atoms are surrounded octahedrally by water molecules. From X-ray data on the heptahydrate [6], which also yields sixfold coordination of the sodium atoms here and monomeric $[\text{SiO}_2(\text{OH})_2]$ tetrahedra, some structural similarity between the octa- and the heptahydrate is concluded. This might be responsible for

Fig. 8. Sketch of individual anion-units $[\text{Si}(\text{OH})_2\text{O}_2]^{2-}$ and their mutual interlinkage from hydrogen bonding. Silicate hydrates show an increasing tendency for chain formation with a decreasing number of hydrate water molecules per silicate phase $\text{Na}_2\text{H}_2\text{SiO}_4 \cdot n\text{H}_2\text{O}$ ($n = 4, 5, 7, 8$). Unique $[\text{Si}(\text{OH})_2\text{O}_2]^{2-}$ endless chains in the tetrahydrate [3] (c) and in the pentahydrate [1] (b) correspond to the distinct melting points of these phases. The octahydrate, on the other hand, shows monomeric $[\text{SiO}_2(\text{OH})_2]^{2-}$ anions (a, d). Here, none of the silicate oxygens are hydrogen bonded to each other. Intensive hydrogen bonding is revealed, however, to the water molecules, which coordinate the sodium atoms octahedrally (part of the structure of $\text{Na}_2\text{D}_2\text{SiO}_4 \cdot 8\text{D}_2\text{O}$ from neutron diffraction data [2]). Details of the heptahydrate structure are not available so far.



the closely related melting points of 325 and 323 K, respectively. A more thorough discussion of this relation will be given as soon as the exact positional parameters of the hydrogen atoms in the heptahydrate are available. (Neutron diffraction work is currently under way.)

The two lower members in the hydrate series, $\text{Na}_2\text{H}_2\text{SiO}_4 \cdot 4 \text{H}_2\text{O}$ and $\text{Na}_2\text{H}_2\text{SiO}_4 \cdot 5 \text{H}_2\text{O}$, show the monomeric anion type $[\text{SiO}_2(\text{OH})_2]^{2-}$ as well. These tetrahedra show hydrogen bonding to each other, however, forming endless chains of different patterns (Fig. 8). This feature, and the corresponding differences in the $\text{Na}(\text{O}, \text{H}_2\text{O})_n$ coordination, might account for the considerably lower melting temperatures of the tetrahydrate (351 K) and the pentahydrate (341 K). In Fig. 7 the outstanding position of the tetrahydrate from the rest of the members of the hydrate series is shown to be due to space filling mechanisms.

Complete thermal data from DSC experiments are shown in Table 1. Melting points and enthalpies of fusion are given for the complete set of hydrate phases $\text{Na}_2\text{H}_2\text{SiO}_4 \cdot n \text{H}_2\text{O}$ ($n = 4, 5, 7, 8$) under closed system or open system conditions for single crystals and polycrystalline material, 25–50 μm in size. Heating rates and other experimental conditions which

TABLE 1

Thermal properties of disodium dihydrogensilicate hydrates: Melting points, glass points, heats of fusion, entropies of fusion (e.s.d.'s ~ 6% for the heats and entropies of fusion)

Compound	M.p. (K)	T_g (K)	ΔH (kJ mol ⁻¹)	Δs (kJ mol ⁻¹ K ⁻¹)	Condition
<i>Single crystals</i>					
$\text{Na}_2\text{H}_2\text{SiO}_4 \cdot 4 \text{H}_2\text{O}$	365		50	0.139	open system
	351	264	49	0.141	closed system
$\text{Na}_2\text{H}_2\text{SiO}_4 \cdot 5 \text{H}_2\text{O}$	346		57	0.167	
	341	255	56	0.166	
$\text{Na}_2\text{H}_2\text{SiO}_4 \cdot 7 \text{H}_2\text{O}$	326		71	0.219	
	325	234	69	0.214	
$\text{Na}_2\text{H}_2\text{SiO}_4 \cdot 8 \text{H}_2\text{O}$	326		75	0.229	
	323	227	71	0.221	
<i>Polycrystalline samples (25–50 μm)</i>					
$\text{Na}_2\text{H}_2\text{SiO}_4 \cdot 4 \text{H}_2\text{O}$	334		87	0.262	
	349	265	52	0.149	
	346		37.3	0.1845	Gould et al. [4]
$\text{Na}_2\text{H}_2\text{SiO}_4 \cdot 5 \text{H}_2\text{O}$	323		88	0.275	
	340	254	52	0.154	
	336		42.0	0.1249	
$\text{Na}_2\text{H}_2\text{SiO}_4 \cdot 7 \text{H}_2\text{O}$	313		91	0.291	
	325	254	52	0.173	
	322		53.1	0.1249	
$\text{Na}_2\text{H}_2\text{SiO}_4 \cdot 8 \text{H}_2\text{O}$	316		99	0.313	
	323	227	63	0.195	
	322		59.6	0.1276	

might affect individual runs were consistent with ideal conditions. These are given by single-crystal quality runs under closed system conditions. The providing of closed system conditions helps to prevent serious deviations from accurate data. Open system conditions, however, favour strong discrepancies in values of melting points as well as in values of enthalpies of fusion, differences increasing with increasing melting temperatures of individual hydrate phases (Figs. 9, 10).

Extreme peak shape deformation is shown by polycrystalline samples as compared to single crystal data under open system conditions (Fig. 4). Systematic lowering of melting temperatures is found here, yielding differences as high as 7 K in the case of the tetrahydrate and systematic reducing of the onset temperatures and flattening of the melting peaks. Enthalpies of fusion are even more strongly affected. ΔH -values show almost doubling in the case of open system conditions for the lower member hydrates ($n = 4, 5$). There is a serious problem, however, in recommending phase analysis of hydrate mixtures to be achieved by systematic DSC studies [4]. Any leakage of the sample container, even micro-fissures lowering the effective pressure of equilibrium to a small amount, might cause a considerable shift of the set point of the melting peak. Peak shape analysis would become extremely difficult, especially under industrial conditions serving for product control analysis. A difference in melting point of 2 K between the

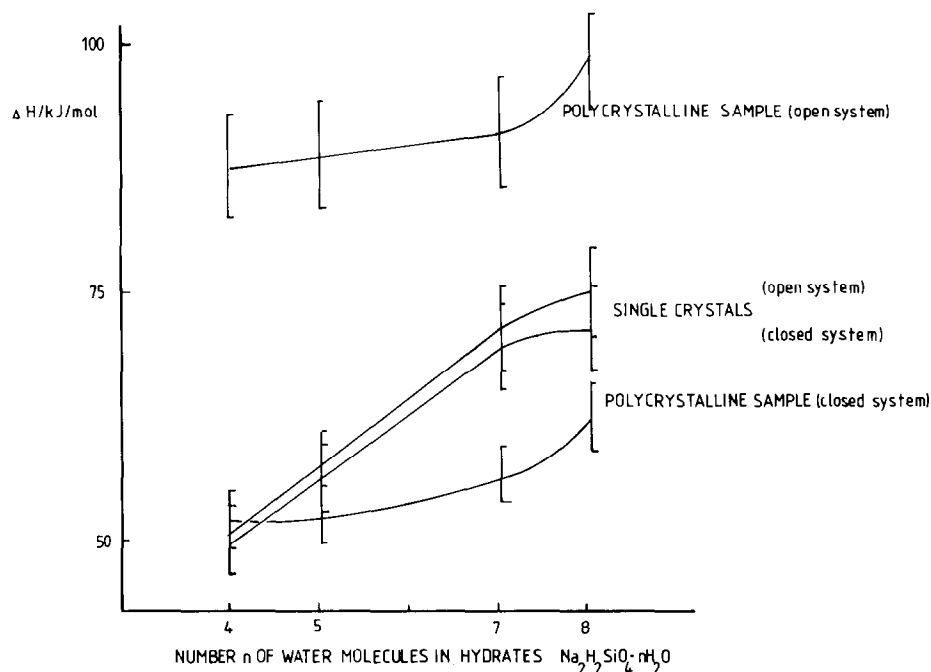


Fig. 9. Enthalpy of fusion (ΔH kJ mol⁻¹) vs. number, n , of water molecules in hydrates $\text{Na}_2\text{H}_2\text{SiO}_4 \cdot n\text{H}_2\text{O}$ (data from Table 1). System conditions (open/closed) definitely affect the ΔH values of polycrystalline samples as obtained from DSC experiments.

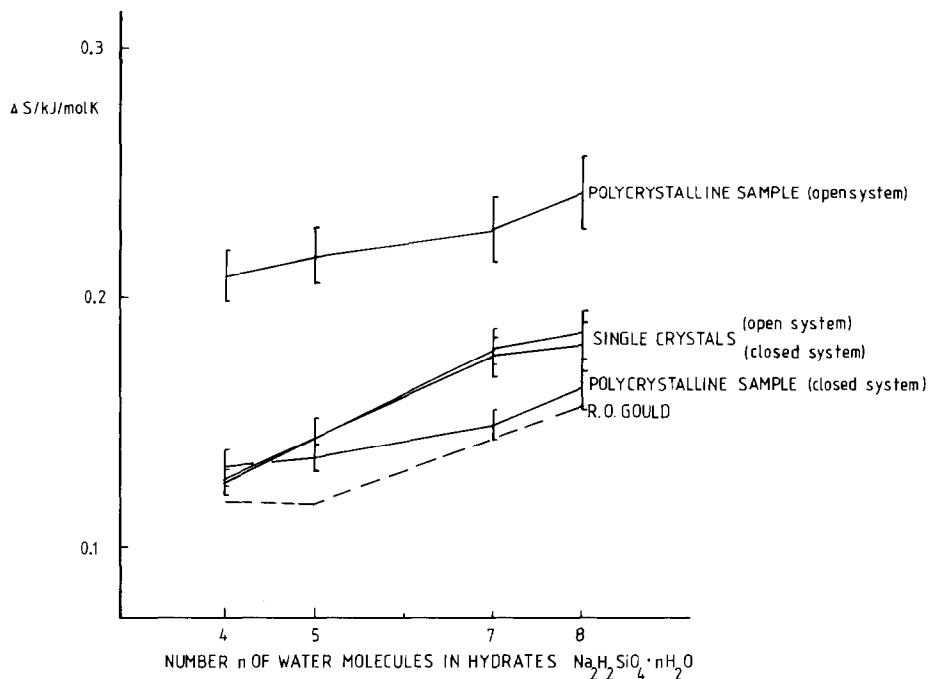


Fig. 10. Entropy of fusion ($\Delta S \text{ kJ mol}^{-1} \text{ K}^{-1}$) of disodium dihydrogen silicates $\text{Na}_2\text{H}_2\text{SiO}_4 \cdot n \text{H}_2\text{O}$ vs. number, n , of hydrate water molecules as obtained from DSC experiments under different conditions. Data from Gould et al. [4] are given for comparison.

octa- and the heptahydrate and employment of silver- or gold-metal capsules for the one way DSC procedures will hardly account for DSC measurement serving as a standard technique in phase analysis. The expenditure for providing exact or reproducible melting data is fairly high. Employing copper pans and lids, for example, considerably increases the number of arbitrarily incorrect data as compared to noble-metal containers.

The data of Table 1 scarcely agree with values of enthalpies of fusion as recently given by Gould et al. [4]. Melting points also show systematically higher numbers in our single crystal/closed system experiments yielding average differences of 3–5 K.

ACKNOWLEDGEMENT

We thank the Deutsche Forschungsgemeinschaft for financial support.

REFERENCES

- 1 P.P. Williams and L.S. Glasser, *Acta Crystallogr., Sect. B*, 27 (1971) 2269.
- 2 R.L. Schmid, J. Felsche and G. McIntyre, *Acta Crystallogr., Sect. C*, (1984) in press.
- 3 R.L. Schmid, J. Felsche and G. McIntyre, *Acta Crystallogr., Sect. C*, (1984) in press.
- 4 R.O. Gould, B.M. Lowe and N.A. MacGilp, *Thermochim. Acta*, 14 (1976) 299.
- 5 G. Chiari and G. Ferraris, *Acta Crystallogr. Sect. B*, 38 (1982) 2331.
- 6 L.S. Glasser and P.B. Jamieson, *Acta Crystallogr., Sect. B*, 32 (1976) 705.